

ADSORPTION PROCESS OF MOLECULARLY IMPRINTED SILICA FOR EXTRACTION OF LACTOSE FROM MILK

A. L. Balieiro¹, R. A. Santos¹, M. M. Pereira³, R. T. Figueiredo¹, L. S. Freitas²,
O. L. S. de Alsina¹, A. S. Lima¹ and C. M. F. Soares^{1*}

¹Institute of Technology and Research, Tiradentes University,
Av. Murilo Dantas 300, 49032-490, Sergipe, Brazil.
E-mail: cleide.soares@pq.cnpq.br

²Department of Chemistry, Federal University of Sergipe, Rod. Marechal Rondon s/n,
Jardim Rosa Elze, CEP: 49100-000, São Cristóvão - SE, Brazil.

³Department of Chemistry, (CIECO), Aveiro University, 3810-193, Aveiro, Portugal.

(Submitted: October 2, 2014 ; Revised: March 6, 2015 ; Accepted: March 10, 2015)

Abstract - In Brazil, about 25–30% of the population has some degree of intolerance to lactose, a disorder associated with the inability of the body to digest lactose due to a disability or absence of the enzyme lactase. The goal of this study was to evaluate the performance of adsorption of lactose from fresh milk using a fixed bed column of molecularly imprinted polymer (MIP). The polymeric material was characterized using Scanning electron microscopy (SEM) analysis, thermal analysis (e.g., differential scanning calorimetric (DSC) and thermogravimetric analysis (TGA), Fourier Transform Infrared Spectroscopy (FTIR), and the method of Braunauer, Emmet and Teller (BET). The adsorption column dynamics and performance were studied by the breakthrough curves using a 2⁴⁻¹ fractional factorial design. The chemical and structural characterization of the pure matrix and imprinted polymers confirmed the molecularly imprinted polymer (MIP) imprinted with lactose. The highest capacity was 62.21 mgg⁻¹, obtained at 307.1 K and a flow rate of 12.5 mL.min⁻¹, with central point conditions, 320.1 K and 9 mL.min⁻¹, with an average value of 50.9 mg.g⁻¹. The results indicate that the molecularly imprinted polymer is efficient.

Keywords: Adsorption; Lactose; Molecularly imprinted polymers; Nanotechnology.

INTRODUCTION

Lactose is one of the carbohydrates in milk. The consumption of more than 20–50 g of lactose on an empty stomach by lactase-deficient individuals causes symptoms of lactose intolerance. Lactose, which is not absorbed in the small intestine, passes into the colon in individuals without the ability to digest it (Brown-Esters *et al.*, 2012). Milk is a typical oil-in-water (o/w) emulsion, with fat globules, sugar and proteins (Manzi and Pizzoferrato, 2011). Therefore, new technologies have been developed for the production of milk products with low lactose content in order to

satisfy the need for people suffering from lactose intolerance (Relpius, 2008). Different methods have recently been proposed in order to remove lactose from milk, as such lactose hydrolysis, capillary electrophoresis, ultrafiltration, and ion-exchange chromatography (Navarro *et al.*, 2014; Bargeman, 2003; Marín-Navarro *et al.*, 2014; Harju, 2007; Mohammad *et al.*, 2012; Oliveira *et al.*, 2014). Other studies have shown the feasibility of using the molecular recognition ability of molecularly imprinted polymers (MIPs) in processes such as adsorption using polymer or silica-based imprinted materials for proteins, polysaccharides and nucleic acids as templates (Li *et al.*,

*To whom correspondence should be addressed

2014; Escobar and Santos, 2014; Dickert and Lieberzeit, 2006; Turner *et al.*, 2006; Bossi *et al.*, 2007; Bergmann and Peppas 2008; Kryscio and Peppas, 2012; Whitcombe *et al.*, 2011).

One potential approach for producing silica-based imprinted materials is the sol-gel process. In this strategy, the template reacts with the precursor (e.g., tetraethylorthosilicate – TEOS), which produces a silica network with the encapsulated molecule such as cholesterol or a protein (Li *et al.*, 2014; Soares *et al.*, 2007). This method has been successfully applied for the direct synthesis of an imprinted mesoporous adsorbent for selective recognition of biomolecules (Morais *et al.*, 2013). In recent years, the potential for molecularly imprinted polymers (MIPs) to impact on these technological areas has stimulated intense activity at hundreds of research centres and companies across the world in order to capitalize on the attributes of these “smart” materials (Li *et al.*, 2014; Seolatto *et al.*, 2009; Dawson *et al.*, 2012).

From this latter perspective, it seems interesting to use innovative processing for the extraction of lactose from milk using an adsorption process with molecularly imprinted silica. In this technique for adsorption, the process uses molecularly imprinted silica particles that have specific recognition sites for the separation of lactose from multicomponent mixtures. The adsorption process for extraction of lactose from milk has not been studied and new studies with this innovative process are necessary. In the adsorption process with molecularly imprinted silica, recovery is possible. So it is still possible to improve the economic viability of the process by extraction of lactose from milk and lactose recovery.

In this study, we attempted to synthesize a new MIP, MP and MIP-LAC. The materials were prepared through self-hydrolysis, self-condensation, and co-condensation of tetraethoxysilane (TEOS). The structural characteristics and adsorption properties of the polymers, including nitrogen adsorption-desorption analysis, thermogravimetric analysis and scanning electron microscopy, are described and discussed in detail. To evaluate the adsorption of lactose in a fixed bed of the MIP, we used a fractional factorial design (2^{4-1}) to assess the influence of operational variables: temperature, flow rate, particle size and height of the bed column.

EXPERIMENTAL

Materials

Bovine milk samples were obtained from dairy producers in the Basin of Nossa Senhora da Gloria,

located in northeastern Brazil in the western part of the State of Sergipe in the micro-region of the hinterland of the San Francisco River. They were stored under refrigeration at the Food Research Laboratory of the Institute of Research and Technology.

The silane precursor tetraethylortosilicate (TEOS) from Sigma Chemical Co. (St. Louis, MO) was used without further purification as a precursor for producing the molecular imprinted polymer. Ethanol (pure>99%), ammonia (pure>28%), HCl (pure>36%), and lactose (pure>99%) were purchased from Sigma Aldrich. Solvents were standard laboratory grade and other reagents were purchased either from Aldrich Chemical Co. (Milwaukee, WI) or from Sigma Chemical Co.

Synthesis of the Pure Matrix and Imprinted Polymers

The MP, MIP, and MIP-LAC were prepared using the sol-gel process and tetraethoxysilane (TEOS) as raw material. For MIP and MIP-LAC, the TEOS and the target molecule (lactose) were dissolved in ethanol utilizing methodology previously established by Soares *et al.* (2007), with adaptations. The steps were as follows: pre-hydrolysis, hydrolysis, solid material synthesis through gelation for 18 h, extraction (washing) and drying at 277.2 K. In the case of MIP, complete removal of lactose was performed in a washing step, while in the synthesis of MIP-LAC, no removal of the biomolecule (lactose) was performed. For the MP no target molecule (lactose) was included in the process (pre-hydrolysis, hydrolysis, solid material synthesis through gelation for 18 h, washing and drying at 277.2 K) in order to obtain the solids.

Characterization of Lactose, MP, MIP and MIP-LAC

Fourier Transform Infrared Spectroscopy (FTIR)

The solid samples were submitted to Fourier Transform Infrared Spectroscopic analysis (FTIR Spectrophotometer MB-3000). Each sample was mixed with 100 x KBr to prepare the pellets. The spectra were obtained in the wavelength range of 400–4000 cm^{-1} to evaluate the printing of the biomolecule (lactose).

Thermogravimetric Analysis (TGA)

The hydrophobic matrices and the lactose standard were determined by weight loss in a TGA apparatus (TGA-50 Shimadzu Thermogravimetric Analyzer)

over the range of 303–1273.2 K, with a heating rate of 10 K.min⁻¹, using nitrogen as the purge gas and a gas flow of 50 mL.min⁻¹. To eliminate sources of error that could arise from the presence of residual reactants, weight loss was only considered for temperatures above 403.1 K. The percentage of the grafted material was calculated using Equation (1):

$$\text{Grafted material}(\%) = \frac{100(w_i - w_f)}{w_i} \quad (1)$$

in which w_i and w_f are the initial and final weight of the sample, respectively, the first taken at 403.2 K and the latter at 1273.2 K.

Differential Scanning Calorimetry

Thermal behaviour was studied using a Differential Scanning Calorimeter Autosampler System (TA Instruments, New Castle, DE). Approximately 5 mg of the sample was weighed in an aluminium pan under a nitrogen atmosphere and thermograms were recorded using a heating rate of 10 K.min⁻¹ up to a temperature of 773.1 K. Glass transition values (T_g) were taken as the midpoint of the transition in the second scan of the DSC thermograms.

Scanning Electron Microscopy (SEM)

The morphology of the samples of MP, MIP, standard lactose LAC and MIP-LAC was investigated using scanning electron microscopy. Carrier particle size and surface roughness were visually assessed using a scanning electron microscope (SEM; Hitachi S4100, Zeiss, Germany). Prior to SEM, approximately 20 nm of platinum were deposited onto the particles via sputter coating.

Specific Surface Area and Porous Properties

The surface areas of the LAC, MP, MIP, and MIP-LAC were calculated using the Brunauer–Emmett–Teller method. Pore volume and average pore diameter were calculated based on the model developed by Barret, Joyner and Halenda (BJH) for microporous samples by the t-method. Surface areas were evaluated according to their N₂ adsorption at 77K using the BET apparatus software (Model NOVA 1200e – Surface Area & Pore Size Analyzer, Quantachrome Instruments – version 11.0). Prior to analysis, samples were submitted to a thermal treatment at 393.1 K for 48 h to eliminate any water existing within the pores of the solids.

Methods

Analysis Determination Lactose

The calibration curve and measurement of lactose were performed by High Performance Liquid Chromatography (HPLC) using a liquid chromatography (Shimadzu), ELSD detector (ELSD-LT II) and software (program Shimadzu LC Solution version 4.5.). The concentration of the standard solution of lactose ranged from 30 to 300 ppm. For processing the data, the analytical column used was a Luna NH₂ (250mm x 4.6 mm) (Phenomenex). The mobile phase consisted of acetonitrile and ultrapure water (50:50) at a flow rate of 1.5 mL.min⁻¹, with an analysis time of 10 min. For the determination of lactose from milk samples: 30 µL samples were diluted in a 2 mL volumetric flask in ultrapure water and then the samples were filtered through a 0.45 Millipore membrane and subsequently injected into the equipment (Bühling and Hinrichs, 2011).

Adsorption Experiments

The experiment was conducted under continuous flow in a jacketed column packed with the MIP adsorbent. The glass column was 20 cm in length with an internal diameter of 2.5 cm. The jacket input and output were connected to a thermostatic bath to guarantee constant control of temperature in the column. At the base of the column sintered glass wool was used to avoid that small particles of the adsorbent contaminated the remainder of the experimental unit. The bed porosity was determined experimentally by pycnometry and was equal to 0.5 ± 0.03. However, it was observed that under the operating conditions a significant compaction of the bed occurred, possibly due to the downward direction of flow. In view of this, we chose to determine the dynamic porosity by direct measurement of the volume of milk retained in the interstices for various operating conditions, yielding a porosity equal to 0.09 ± 0.005. The compacting effect occurred before the start of the experiment during the flooding of the column with water. Thus, throughout the experiment the bed features remained constant (bed height and porosity).

Milk was fed at the top of the column by a peristaltic pump at a controlled flow rate. Aliquots of the effluent were collected at the bottom of the bed at predetermined time intervals and reserved for later analysis by HPLC. The samples were collected until bed saturation or until the lactose concentration in the fluid phase remained constant throughout the column and equal to the feed concentration.

The effect of operational variables on the adsorption of lactose in the packed column was studied by a fractional factorial design (2^{4-1}) with four independent variables (flow rate, temperature, particle size and bed height) and adsorption capacity (q_0) as dependent variable. Three replicates at the centre point were included according to Table 1.

Table 1: Codified and uncoded values of the input factors.

Operating variable	-1	0	+1
X ₁ (temperature, K)	307.1	320.1	333.1
X ₂ (particle size, mesh)	32	42	60
X ₃ (bed height, cm)	7.5	10	12.5
X ₄ (flow rate, mL.min ⁻¹)	3	6	9

The adsorption capacity q , expressed as mg of lactose per g of adsorbent, was obtained from the breakthrough curve for each run by means of Equation (2).

$$\int_0^t \frac{\dot{V}C_0 - \dot{V}C}{C_0} dt = \frac{q_0 m}{C_0} + \frac{\varepsilon \pi D^2}{4} H \frac{C}{C_0} \quad (2)$$

where: \dot{V} - flow rate, ε - porosity, q_0 - adsorption capacity, C_0 - initial concentration, C - final concentration, H - height, m - mass of adsorbent, and t - time.

RESULTS AND DISCUSSION

The aims of our work were to evaluate the performance of lactose adsorption from fresh milk using a fixed bed column of MIP. However, it was necessary to study the structures of the polymers obtained by molecular imprinting in order to evaluate the molecular assembly formed by the inclusion complex of lactose in the polymer used as a template for the molecular imprinting. The structures of LAC and the three polymers MP, MIP, MIP-LAC were characterized by FT-IR spectroscopy, Thermogravimetric analysis (TGA), Differential Scanning Calorimetry (DSC), Scanning Electron Microscopy (SEM) and for the specific surface area and porous structure by N₂ physisorption. Afterward, the imprinting effect of the MIP was studied by analysing the adsorption of lactose in fresh milk using a fixed bed column of the MIP.

Chemical and Structural Characterization of the Pure Matrix and Imprinted Polymers

One of the main aims of the chemical and structural characterization of lactose, the pure matrix and the imprinted polymers was to provide a set of unified criteria or conditions to assist in verifying the potential for imprinting of lactose, together with testing the adsorption capacity of the MIP for lactose. Recently, the relationships between chemical characteristics and imprinting properties have been examined using Fourier transform infrared (FTIR) spectra for biomolecules and polymers before and after imprinting (Ibrahim, *et al.*, 2009; Wanyika *et al.*, 2011).

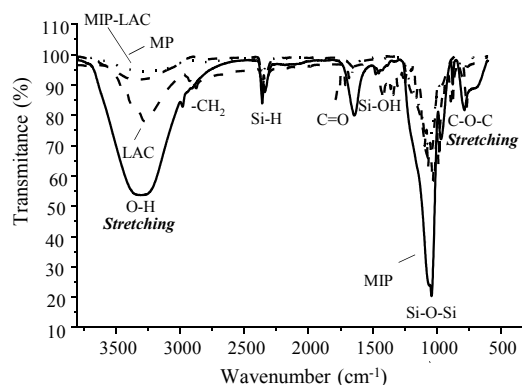


Figure 1: FT-IR spectra of the standard lactose (LAC), pure matrix (MP), molecularly imprinted polymer (MIP), molecularly imprinted polymer with lactose (MIP-LAC).

Characteristic peaks in the FT-IR spectra for lactose in Figure 1 were assigned and compared according to the literature. We observed characteristic bands due to specific forms of lactose (Listiohadi *et al.*, 2009; Kirk *et al.*, 2007; Lei *et al.*, 2010; Islam and Langrish, 2010). The characteristic band for α -lactose appeared at 920 cm⁻¹, and those for β -lactose at 950 cm⁻¹ and 833 cm⁻¹ (Kirk *et al.*, 2007; Listiohadi *et al.*, 2009). According to Lei *et al.*, (2010), the bands present in the spectrum at 2925–2927 cm⁻¹ correspond to methylene (-CH₂) or aromatic compounds, bands at 1150–1030 cm⁻¹ to intermolecular stretching of carbohydrates, bands at 800–1000 cm⁻¹ to carbohydrates, and a band at 3200 cm⁻¹ to intermolecular stretching (Islam and Langrish, 2010). The presence of the C=O group was confirmed by its peak value at 1700 cm⁻¹. It should also be observed that the characteristic stretching and bending frequencies of the C-O-C glycosidic bond (the bond

linking the two sugar moieties) were present in both spectra (~ 1100 and ~ 800 cm^{-1}) (Crisp *et al.*, 2010).

The spectrum recorded in the pure matrix (MP) presents bands typical of the groups present in both polymeric networks on the surface. In the region around 3400 cm^{-1} are stretches of silanol hydroxyl groups and also of molecules adsorbed on the surface of the oxide through hydrogen bonding. A broad and intense band between 3300 and 3700 cm^{-1} is associated with Si-OH groups and -OH stretching in H-bonded water, due to adsorption of water molecules on the surface of the pore channels (Hu *et al.*, 2005). The band in the 1630 cm^{-1} region for deformations of water molecules can confirm the presence of water. The higher intensity of the broad band at 3435 cm^{-1} can be attributed to the water molecules in the space of the molecularly imprinted silica and molecularly imprinted polymer (MIP). This intensity was lowest for standard lactose (LAC), pure matrices (MP) and molecularly imprinted polymer with lactose (MIP-LAC), shown in Figure 1. The stretching vibration of the Si-OH groups was observed and the strong 1100 cm^{-1} bands were ascribed to Si-O-Si stretching vibrations, while the bands at 1628 , 970 , 804 and 460 cm^{-1} were attributed to SiO-H bending, Si-OH bending, SiO-H symmetrical stretching and Si-O bending vibrations, respectively (Wanyika *et al.*, 2011). Water bands in the region 1630 cm^{-1} were attributed to deformation of hydroxyl groups, while the bands at 1494 , 1439 and 1402 cm^{-1} were assigned to C-H deformation in the -CH₂ of an ethoxy group (Ibrahim *et al.*, 2009). The O-CH₂ and CH₃ vibrations observed at 1464 cm^{-1} and a band at 1260 cm^{-1} are due to the C-O-C asymmetric stretching vibration. The presence of these stretches indicates that the molecular imprinting reaction was actually consummated. Similarly, these bands are also present in the MIP-LAC polymer with less intensity, possibly due to the presence of some of the target molecules (LAC) still in the polymer.

The peak at about 960 cm^{-1} , which corresponds to the stretching vibration of Si-O-H bonds, is very pronounced in the MIP sample, and this could be explained by the existence of a larger number of surface O-(H...H₂O) groups bound to Si (Nikolić *et al.*, 2010). Around 1700 cm^{-1} there are bands which are missing in MP, regarding C=O group stretches, which are strongly present in the MIP. The presence of these stretches possibly indicates that the molecular imprinting was actually consummated.

The change in intensity of the band in the 3700 - 2900 cm^{-1} region (characteristic of the stretching of silane groups, Si-OH) and the bands in the 1630 -

1110 cm^{-1} region for siloxane groups in Figure 1 for MIP were obviously caused by lactose.

Thermogravimetric Analysis (TGA)

Silica-based materials are extremely rigid due to the high degree of cross-linking found in the SiO₂ network. This property is very important in the design and synthesis of MIPs, as both the size and shape of the cavities created by the template must be retained after removal of the template. The high thermal stability of the sol-gel derived material provides an easy way to remove the template molecule using the high temperature calcination method (Lee *et al.*, 2010). Figure 2 shows the TG curve and DTA lactose standard analyzed in a N₂ atmosphere.

After examining the data, the Tg of lactose is normally seen in the temperature range of 379.1 - 442.1 K. This lower Tg temperature was believed to be caused by the plasticization of the lactose by water, which is not lost during the fast scan. After the glass transition, an exotherm associated with recrystallization is observed, and this is followed by two melting events. The two peaks are associated with the two forms of lactose that recrystallize from the post-Tg material. The first peak is the melting of anhydrous α -lactose, and the second peak is associated with β -lactose. It is also worth noting that recrystallization of the sample still occurs even at 773.1 K, and there is no loss of resolution of the melting of the two forms of crystalline lactose (Hogan and Buckton, 2000).

As to TGA analysis of the samples, a dehydration occurred between 379.1 and 442.1 K, presumably due to the loss of surface water; melting between 497.5 and 549.1 K and a sequence of three consecutive stages of thermal decomposition of the lactose (exothermic, endothermic and exothermic). The initial decomposition temperature occurred immediately after the fusion. The step of carbonaceous residue formation ended at 913.1 K. A greater weight loss occurred in the second decomposition step, with a percentage close to 63.0% for LAC (Figure 2).

The mass losses of samples of MP, MIP, and MIP-LAC, were determined by thermogravimetric analysis (TGA) according to Figure 3.

The thermal stability of the samples was investigated by TGA analysis, whose results are plotted in Figures 2 and 3 as a function of temperature on the x-axis and percent weight loss on the y-axis. Weight loss occurred in all samples up to 400 K due to the loss of water, as shown in Figures 2 and 3.

It can be seen in Figure 3 that the MIP sample showed a weight loss of only 22% at 473.1 K. Pre-

sumably in this first stage part of this weight loss was due to the loss of surface water and also to the removal of water molecules that were not tightly bound to the silica matrix, in accordance with the literature (Wei *et al.*, 1999; Mukherjee *et al.*, 2009; Wanyika *et al.*, 2011). At two other stages, the loss in weight at higher temperatures was ascribed to loss of surface silanol groups (Wanyika *et al.*, 2011).

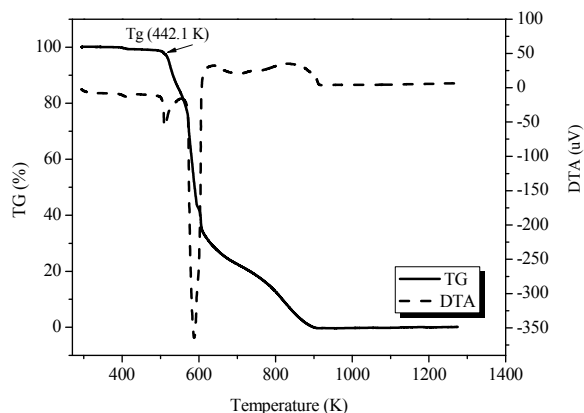


Figure 2: TG and DTA curves of lactose standard analyzed in a N_2 atmosphere.

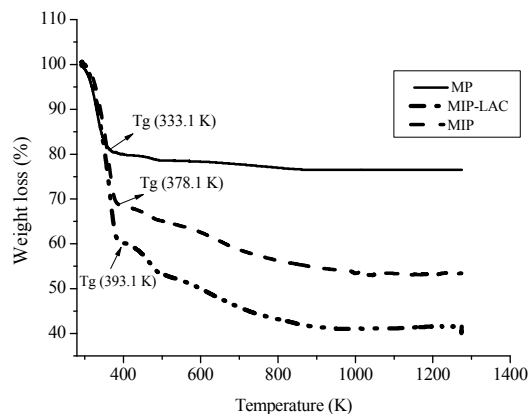


Figure 3: TG curves in an atmosphere of N_2 for the pure matrix (PM), molecularly imprinted polymer (MIP), molecularly imprinted polymer with lactose (MIP-LAC).

The weight of MIP declined sharply between 453.1 K and 473.1 K, which might correspond to degradation of the carbon skeleton. Almost the entire weight was lost at 723.1 K. Analogously, the MIP-LAC had a similar weight loss trend with increasing temperature, until it became stable above 723.1 K with about 96% of the total weight loss. The difference in weight loss between MIP-LAC and MIP (58% and 46%, respectively), was possibly caused by the removal of the target molecule (lactose), con-

firmed the success of the molecular imprinting. Similar results were found by Mao *et al.* (2011) in evaluating a novel composite of graphene sheet/Congo red-molecular imprinted polymers (GSCR-MIPs).

In general, the three weight loss regimes observed in the TGA profiles most likely originate from: (i) moisture, due to the adsorbed water on the surface of the lactose or MP or MIP-LAC or MIP (293.1–353.1 °C); (ii) loss of lactose or MIP-LAC (373.1 at 473.1 K); (iii) decomposition plus dehydration of surface hydroxyl groups in the MP or MIP-LAC or MIP (>523.1 K) (Guo *et al.*, 2003; Suteewong *et al.*, 2012).

Differential Scanning Calorimetry (DSC)

The most common measurement of amorphous structures involves analysis of the glass transition by DSC. It is important to examine both the size of the transition in heat flow or heat capacity units and the temperature (T_g) at which it occurs. The size of the transition provides quantitative information about the amount of amorphous structure in the sample, and the temperature identifies the point where there is a dramatic change in its physical properties. Figure 4 shows an overlay of a number of DSC analyses from 273.1 to 773.1 K for lactose and the polymers. In each case an excellent glass transition was obtained.

The thermal curve of lactose was characterized by a strong dehydration endotherm with an onset temperature of 415.3 K, a peak temperature of 417.6 K, and an enthalpy of dehydration equal to 149.7 J.g^{-1} . This was followed by the lactose decomposition endotherm near 493.1 K. The DSC profile for lactose is shown in Figure 4. Theoretically, the thermal curve should only consist of the decomposition endotherm near 509.1 K, but the sample appears to contain a small contamination of the α -monohydrate phase as there is a residual endothermic peak near 401.1 K. Based upon the measured dehydration enthalpy of 18.9 J.g^{-1} , the β -lactose contains about 12.6% α -monohydrate phase, (Kaialy *et al.*, 2012).

Concerning the decomposition steps, the DSC analysis of lactose initially presented a peak corresponding to endothermic dehydration at 409.6 K with a heat of 13.2 J.g^{-1} , followed by melting at 513.8 K with a heat of 103.3 J.g^{-1} , and by two exothermic peaks at 578.1 and 605.1 K with heats of 34 and 67 J.g^{-1} , respectively (Brittain and Blaine, 2007).

With the pure matrix (MP), a temperature of 338.7 K was found to cause a loss of mass of the water bound on the silica surface by weak hydrogen bonds. With increasing temperature, the material initiated a second loss of mass, which was attributed to

the condensation of silanol groups at a temperature of 479.1 K. At temperatures above 473.1 K, further loss of water occurred due to condensation of silanol groups and siloxanes (Figure 4). The porous silica with lactose presented a higher water content when compared with the porous silica MIP, in accordance with what was observed in the endothermic transition.

The sample of pure matrix (MP) showed only one endothermic transition, with a peak temperature of 338.1 K and an enthalpy of 364.3 J.g⁻¹. The sample containing lactose (MIP-LAC) showed a first endothermic peak temperature of 423.1 K and an enthalpy of 764.3 J.g⁻¹, associated with decomposition of organic matter and loss of water. However, the main change caused by the presence of lactose in the matrix was related to the increase in energy of the endothermic peak, (764.3 J.g⁻¹/423.1 K).

This behaviour could be associated with the loss of water still present in the sample as so-called “water of hydration,” and strongly present in the lattice, since it is possible that water can be maintained on the surface of silica gel by different forces of interaction: “dispersion forces” (e.g., physically bounded water), “polar forces” (e.g., hydrogen bounded water), or by “chemical forces” (e.g., silanol groups that condense to form siloxane bonds with the release of water) (Soares *et al.*, 2004).

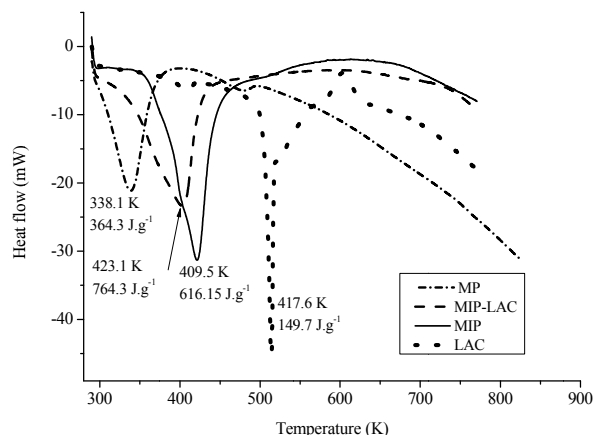


Figure 4: DSC curves in an inert atmosphere of nitrogen for lactose (LAC), pure matrix (MP), molecularly imprinted polymer (MIP) and molecularly imprinted polymer with lactose (MIP-LAC).

We observed an endothermic peak, which can be attributed to evaporation of molecular adsorbed water on the gel surface; moreover, the endothermic peak intensity was greater for the curve of MIP-LAC, possibly due to the presence of the lactose. The information obtained in the DSC, TG and DTA curves for lactose (LAC), pure matrix (MP), molecu-

larly imprinted polymer (MIP) and molecularly imprinted polymer with lactose (MIP-LAC) confirm the success of the molecular imprinting of lactose into silica, thus obtaining silica-based imprinted material.

Scanning Electron Microscopy (SEM)

The SEM analyses in Figure 5 show clearly the morphologies of the mesoporous silica obtained, including MP, MIP, and MIP-LAC. It can be observed from the micrographs that the materials have a porous structure characteristic of this type of material, which can even be observed in the SEM literature for silica gel (Oliveira, 2009). For illustration, the forms of lactose particles are dense and have a rough surface (Figure 5(a)).

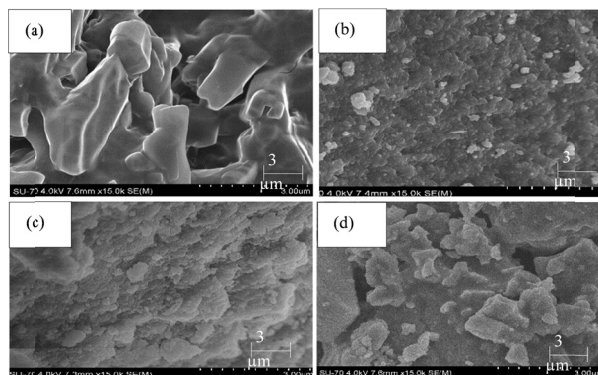


Figure 5: SEM micrographs of (a) LAC; (b) MP; (c) MIP-LAC and (d) MIP.

In Figure 5(b) aggregates of varying sizes are present, suggesting uniformity in the particle sizes involved. On the basis of several reports in the literature, the presence of pores in the clear surface structure favours accessibility to the sites of the molecular imprint (Hua *et al.*, 2011; Pradhan *et al.*, 2009). Moreover, widely dispersed microparticles were observed, as well as heterogeneity with regard to particle shape, with predominantly spherical shapes of different sizes and spongy textures molecularly printed with lactose (Figure 5(c)). However, in the micrographs of the MIP there are voids due possibly to the modification of the surface after removal of the lactose (target molecule) (Figure 5(c)). Thus, the micrographs of the MIP and of MP or MIP-LAC are entirely different and these differences are probably due to the molecular imprinting of lactose (Figure 5(b)-(d)).

Specific Surface Area and Porous Properties

The nitrogen adsorption/desorption BET isotherm is a multilayer adsorption model that allows an esti-

mate to be made of the number of adsorption sites in a monolayer and of the specific surface area of the sample. The molecularly imprinted polymer (MIP) generates binding cavities that are complementary to the original template in the pure matrix (MP) or the polymer molecularly imprinted with lactose (MIP-LAC). The structural parameters of the mesoporous silica obtained from the N₂ adsorption data are shown in Table 2.

Table 2: Structural parameters of the mesoporous silica obtained from the N₂ adsorption data.

Sample	Surface area (m ² .g ⁻¹)	^a Pore volume (cm ³ .g ⁻¹)	Pore diameter (Å)
MIP-LAC	437.8	0.6	50.0
MP	301.8	0.9	109.5
MIP	464.2	1.9	150.0

^a Pore volume calculated from nitrogen desorption.

Table 2 shows materials with pores diameter between 50 to 150 Å. The pure matrix showed a low pore volume (0.9 cm³.g⁻¹) and a narrow distribution of pore size (109.5 Å, Table 2) (Leofanti, 1998). After the addition of lactose, the matrix had a pore volume of (0.5 cm³.g⁻¹), while the MIP pore volume (1.9 cm³.g⁻¹), surface area and pore size significantly increased in comparison with the MIP-LAC sample (0.6 cm³.g, 50 Å, 437.8 m².g⁻¹), (MIP). Higher values were found by (Tominaga *et al.*, 2005), where the authors synthesized mesoporous silica (MPSi) as a novel type of inorganic filler for polyether-based electrolytes, characterized the effect of the addition on ionic conduction and found a superficial area of 829 m².g⁻¹. An inferior pore size was found by Qu *et al.* (2006), who reported values of 2.7 and 2.1 nm.

In addition, Table 2 shows that the BET surface area gradually increases in matrices printed with lactose in the polymer structure, directly affecting

the porosity of the final product.

The BET surface areas of our materials (e.g., 464.2 m².g⁻¹) were comparable to those reported elsewhere, i.e., 594 m².g⁻¹ (Qu *et al.*, 2006) for a similar material prepared using TEOS as the silica source. However, the pore size and pore volume of our material (e.g., 150 Å and 1.8 m³.g⁻¹, respectively) were extremely high compared to those reported for a similar mesoporous silica (e.g., 3.2 nm and 0.6 m³.g⁻¹, respectively) made using TEOS (Hossain and Sayari, 2008).

Therefore, the chemical and structural characterization of the pure matrix and imprinted polymers confirmed that the polymer was MIP with lactose. Next, we evaluated the adsorption of lactose from fresh milk using a fixed bed column packed with the MIP.

Adsorption of Lactose in a MIP Fixed Bed

The fixed bed adsorption process was studied in the non-steady state, with fresh milk and constant flow rate. In this way, the specific interactions between analyte (lactose) and sorbent MIP revealed the adsorptive capacity in the process.

In Table 3 it can be observed that the highest adsorptive capacity of the MIP adsorbent was 62.2 mg.g⁻¹, obtained in test E5, with a 12.5 cm bed, flow rate of 9 mL.min⁻¹, temperature of 307.1 K and particle size corresponding to 32 mesh. This corresponded to central point conditions (height 10 cm, 6 mL.min⁻¹, 320.1 K and 42 mesh) with an average value for the adsorptive capacity of 50.9 mg.g⁻¹. Notice the good reproducibility of the central point triplicates. The lowest adsorptive capacity was found in the E6 and E7 runs, 9.5 mg.g⁻¹ and 7.2 mg.g⁻¹, respectively, both with 12.5 cm bed height and a 3 mL.min⁻¹ flow rate, whereas the temperature was 333.1 K and 32 mesh in E6 and 307.1 K and 60 mesh in E7.

Table 3: Lactose adsorption experiments in a MIP fixed bed.

Assays	Bed height (cm)	Flow rate (mL.min ⁻¹)	Temperature (K)	Particle size (mesh)	Input lactose concentration (mg.L ⁻¹)	Adsorption Capacity (mg.g ⁻¹)
E1	7.5	3	307.1	32	21779	28.0
E2	7.5	9	333.1	32	21746	37.6
E3	7.5	9	307.1	60	20765	47.5
E4	7.5	3	333.1	60	19382	26.4
E5	12.5	9	307.1	32	19518	62.2
E6	12.5	3	333.1	32	12772	9.5
E7	12.5	3	307.1	60	13906	7.2
E8	12.5	9	333.1	60	19518	24.3
E9	10.0	6	320.1	42	21806	52.4
E10	10.0	6	320.1	42	32454	50.6
E11	10.0	6	320.1	42	21751	49.5
E5*	12.5	9	320.1	32	19518	31.8

(*) Experiment with non-imprinted polymer

Because fresh milk was used in the experiments, the lactose input concentration was an uncontrolled variable. The results in Table 3 could imply that the input concentration of lactose in the milk may influence the adsorption capacity. This suggests that the mass transfer coefficients in the adsorbent in the fixed bed are concentration dependent, as the removal rate and adsorption capacity were affected by a change in concentration. This phenomenon had already been observed by other researchers, who evaluated the removal of Cr(III) in fixed bed columns in batch reactors using as adsorbent zeolite NaX (Barros *et al.*, 2004; Silva *et al.*, 2002; Ostroski, *et al.*, 2011). Moreover, it is clear from the results in Table 3 that the operational conditions have a large effect on the bed performance. In order to assess the extent and significance of these influences, a statistical approach was used to determine the effect of each variable, as well as the form and effect of each variable and their interactions. Typical values for the adsorption of lactose show the main significant factors in adsorption. The Pareto graph or bed adsorption capacity is shown in Figure 6.

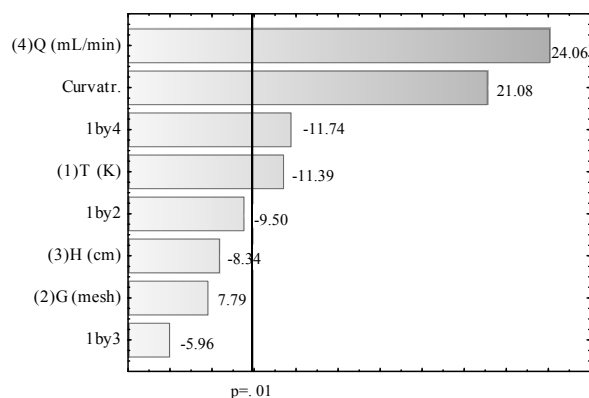


Figure 6: Pareto chart of standardized effects for the adsorption of lactose in the MIP.

It can be observed from the Pareto diagram that the bed height and particle size are not significant variables for the bed adsorptive capacity at the 99% confidence level. The temperature (X_1), flow rate (X_4) and interaction of temperature with flow rate ($X_1:X_4$) were significant. The variable that most influenced the adsorption of lactose was the flow rate. The positive sign in the variable means that passing from level -1 (3 mL.min⁻¹) to level +1 (6 mL.min⁻¹) increased the response factor; that is, the adsorption capacity increased with the flow rate. In contrast, the effect of temperature and its interaction with the flow rate are negative; an increase in this variable diminishes the bed capacity. These results were not expected, because it was anticipated that the adsorption

capacity would be dependent on the mass transfer mechanism. This could be due to elution by the milk flowing across the column causing the partial desorption of lactose, which becomes more important for longer residence times. This was confirmed in long runs, where the effluent concentration was higher than the input lactose concentration.

Upon completion of the analysis of the experimental results obtained from the evaluation of the response surface (Figure 7), the interaction between temperature and flow rate can be observed such that, when the temperature is reduced and the flow rate is increased, the adsorption capacity also increases, justifying that these variables had significant influence on the adsorption capacity of lactose.

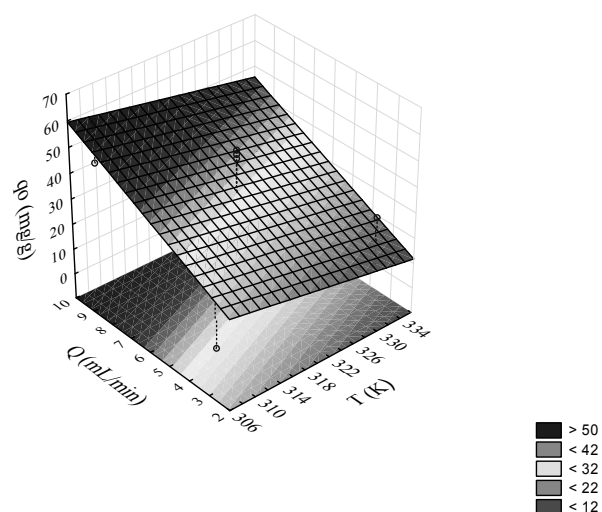


Figure 7: Response surface showing the adsorption capacity in relation to flow and temperature variables.

Selective recognition studies of lactose were evaluated in Figures 8(a) to 8(c), in the illustrated breakthrough curves for the pure matrix (8a), the central point run (8(b)) and optimal conditions with higher adsorption capacity 8(c).

From Figure 8(b) and (c) it can be observed that the MIP breakthrough curves present a region of constant output concentrations, with $C/C_0=8.7$ at $t=7$ min (b) and $C/C_0=4.7$ at $t=4.2$ min (c), respectively, followed by a region where C/C_0 increases until bed saturation. This behaviour was also observed in the other runs performed with MIP adsorbent, unlike the experiment with the unprinted polymer, which did not present a constant output concentration plateau. This difference between the MIP and pure matrix breakthrough curves could be due to a preferential distribution of the sites of specific recognition in more accessible positions within the adsorbent particles of the MIP, which could be responsible for the presence of the plateau region. From these studies it

is possible to operate the column by choosing appropriate operational conditions of flow rate and temperature, for systems of fixed bed adsorption depending on the level of lactose final concentration.

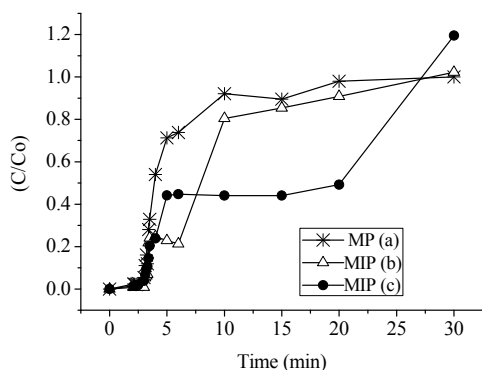


Figure 8: Breakthrough curves for lactose adsorption in fixed bed: (a) MP : non- imprinted polymer: T= 307.1 K; Q=9 mL.min⁻¹; H= 12.5 cm; d= 32 mesh; (b) MIP: T= 320.1 K; Q= 6 mL.min⁻¹; H=10 cm; d=42 mesh; (c) MIP: T=307.1 K; Q=9 mL.min⁻¹; H=12.5 cm; d=32 mesh.

In fact, Figure 8 suggests that it is possible to obtain 100% lactose removal during 3 min, 80% between 3 and 6 min for the MIP (b) conditions or 60% for the MIP (c) conditions. These considerations on a laboratory scale suggest that it would be advantageous to execute the column adsorption process and lactose recovery on a large scale.

The results obtained for the breakthrough curves show that an increase in feed flow rate implies a larger volume of solution per unit time passing through the column, thus providing a shorter operation time, i.e., the adsorbent will saturate faster with increasing flow rate, as can be seen in Figure 8.

The experimental matrix and results for adsorption capacity are shown in Table 3. It can be seen from this table, comparing experiments E5 and E10, that the molecular impression leads to a higher adsorptive capacity of the modified polymer, from 62.2 to 52.4 mg.g⁻¹. This was expected because the presence of specific recognition sites improves the selectivity of the adsorbent. In the present work, the extent of this promising improvement justifies the process and encourages us to pursue further research.

CONCLUSIONS

The methodology employed, based on silica-based matrices prepared by the sol-gel process, was shown to be efficient. We confirmed the molecular

imprint of lactose in the polymer (MIP) by chemical and structural characterization of the pure matrix and the imprinted polymers. The feasibility of lactose removal by adsorption of lactose by the molecularly imprinted polymer was verified and the process was found to be very favourable. The adsorption appeared to require only a relatively short contact time, with the most effective polymer requiring just one hour to reach equilibrium. The results showed that the adsorption process was strongly influenced by temperature and flow. The information obtained in this study can be applied to predict design parameters in systems of fixed bed adsorption. This work is therefore an important step towards the concentration and selective separation of lactose from milk.

ACKNOWLEDGMENTS

We acknowledge financial assistance from the Coordenação de Aperfeiçoamento de Pessoal de Ensino Superior (CAPES), Conselho Nacional de Desenvolvimento Científico e Tecnológico (CNPq) and Financiadora de Estudos e Projetos (FINEP). A.L.B. also acknowledges Professor João Coutinho, CICECO, Universidade de Aveiro, for extending necessary infrastructure and laboratory facilities.

REFERENCES

- Bargeman, G., Separation technologies to produce dairy ingredients, rozdz. 17 w: Dairy processing: Improving quality pod red. In: G. Smith (Ed.), Cambridge, UK, Woodhead Publishing Limited, p. 366-387 (2003).
- Barrett, E. P., Joyner, L. G., Halenda, P. P., The determination of pore volume and area distributions in porous substances. I. Computations from nitrogen isotherms. *Journal of the American Chemical Society*, p. 73, 373-380 (1951).
- Barros, M. A. S. D., Silva, E. A., Arroyo, P. A., Tavares, C. R. G., Schneider, R. M., Suszek, M., Sousa-Aguiar, E. F., Removal of Cr(III) in the fixed bed column and batch reactors using as adsorbent zeolite NaX. *Chemical Engineering Science*, p. 59, 5959-5966 (2004).
- Bergmann, N. M. and Peppas, N. A., Molecularly imprinted polymers with specific recognition for macromolecules and proteins. *Progress in Polymer Science*, 33, p. 271-288 (2008).
- Bossi, A., Bonini, F., Turner, A. P. F., Piletsky, S. A., Molecularly imprinted polymers for the recognition of proteins: The state of the art. *Biosensors and Bioelectronics*, 22, p. 1131-7 (2007).

- Brittain, G. H. and Blaine R. L., α -Monohydrate phase in lactose by differential scanning calorimetry. *Thermal Analysis and Calorimetry*, 68, p. 291-293 (2007).
- Brown-Esters, O., Namara, Mc P., Savaiano, D., Dietary and biological factors influencing lactose intolerance. *International Dairy Journal*, 22, p. 98-103 (2012).
- Bühning, R. S. W., Michel, R., Hinrichs, J., A new liquid chromatography method for the simultaneous and sensitive quantification of lactose and lactulose in milk. *Dairy Science & Technology*, p. 27-37 (2011).
- Crisp, J. L., Dann, S. E., Edgar, M., Blatchford, C. G., The effect of particle size on the dehydration/rehydration behaviour of lactose. *International Journal of Pharmaceutics*, 391, p. 38-47 (2010).
- Dawson, R., Cooper, A. I., Adams, D. J., Nanoporous organic polymer networks. *Progress in Polymer Science*, 37, p. 530-563 (2012).
- Dickert, F., Lieberzeit, P. A., Sensor technology and its application in environmental analysis. *Bioscience*, p. 50-63 (2006).
- Guo, W., Park, J., Oh, M., Jeong, H. W., Cho, W., Kim, I., Ha, C., Copolymer synthesis of highly ordered large-pore periodic mesoporous organosilicas with the aid of inorganic salts. *Chemistry of Materials*, 15, p. 2295-2298 (2003).
- Harju, M., Chromatographic separation of lactose and its applications in the dairy industry. *IDF Symposium Lactose & its Derivatives*, 6, p. 14-16 (2007).
- Hogan, S. E., Buckton, G., The quantification of small degrees of disorder in lactose using solution calorimetry. *International Journal of Pharmaceutics*, 207, p. 57-64 (2000).
- Hossain, K., Sayari, A., Synthesis of onion-like mesoporous silica from sodium silicate in the presence of α , ω -diamine surfactant. *Microporous and Mesoporous Materials*, 114, p. 387-394 (2008).
- Hu, Q., Hampsey, J. E., Jiang, N., Li, C., Lu, Y., Surfactant-templated organic functionalized mesoporous silica with phosphino ligands. *Chemistry of Materials*, 17, p. 1561-1569 (2005).
- Hua, K., Zhang, L., Zhang, Z., Guo, Y., Guo, T., Surface hydrophilic modification with a sugar moiety for a uniform-sized polymer molecularly imprint for phenobarbital in serum. *Acta Biomaterials*, 7, p. 3086-3093 (2011).
- Ibrahim, M. N. M., Sipaut, C. S., Yusof, N. N. M., Purification of vanillin by a molecular imprinting polymer technique. *Separation and Purification Technology*, 6, p. 450-456 (2009).
- Islam, M. I. U., Langrish, T. A. G., An investigation into lactose crystallization under high temperature conditions during spray drying. *Food Research International*, 43, p. 46-56 (2010).
- Kaialy, W., Larhrib, H., Martin, G. P., Nokhodchi, A., The Effect of Engineered Mannitol-Lactose Mixture on Dry Powder Inhaler Performance. *Pharmaceutical Research*, 29, p. 2139-2215 (2012).
- Kirk, J. H., Dann, S. E., Blatchford, C. G., Lactose: A definitive guide to polymorph determination. *International Journal of Pharmaceutics*, 334, p. 103-114 (2007).
- Kryscio, D. R., Peppas, N. A., Critical review and perspective of macromolecularly imprinted polymers. *Acta Biomaterials*, 8, p. 461-73 (2012).
- Lee, S. C., Chuang, F. L., Tsai, Y. L., Chen, H., Studies on the preparation and properties of sol-gel molecularly imprint polymer based on tetraethoxysilane for recognizing sulphonamides. *Journal of Polymer Research*, 17, p. 737-744 (2010).
- Lei, Y., Zhou, Q., Zhang, Y., Chen, J., Sun, S., Noda, I., Studies on the preparation and properties of sol-gel molecularly imprint polymer based on tetraethoxysilane for recognizing sulphonamides. *Journal of Molecular Structure*, 974, p. 88-93 (2010).
- Leofanti, G., Surface area and pore texture of catalysts. *Catalysis Today*, 41, p. 207-219 (1998).
- Li, S. J., Cao, S. S., Whitcombe, M. J., Piletsky, S. A., Size matters: Challenges in imprinting macromolecules. *Progress in Polymer Science*, 39, p. 145-163 (2014).
- Listiohadi, Y., Hourigan, J. A., Sleight, R. W., Steele, R. J., Thermal analysis of amorphous lactose and α -lactose monohydrate. *Dairy Science & Technology*, 89, p. 43-67 (2009).
- Manzi, P., Pizzoferrato, L., HPLC determination of lactulose in heat treated milk. *Food and Bioprocess Technology*, 6, p. 851-857 (2011).
- Marín-Navarro, J., Talens-Perales, D., Oude-Vrielink, A., Cañada, F. J., Polaina, J., Immobilization of thermostable β -galactosidase on epoxy support and its use for lactose hydrolysis and galactooligosaccharides biosynthesis. *World Journal of Microbiology and Biotechnology*, 30, p. 989-998 (2014).
- Mao, Y., Bao, Y., Gan, S., Li, F., Niu, L., Electrochemical sensor for dopamine based on a novel graphene-molecular imprint polymers composite recognition element. *Biosensors and Bioelectronics*, 28, p. 291-297 (2011).
- Mohammad, A. W., Ng, C. Y., Lim, Y. P., Ng, G. H., Ultrafiltration in food processing industry: Review on application, membrane fouling, and fouling control. *Food and Bioprocess Technology*, 5, p. 1143-1156 (2012).

- Morais, E. C., Correa, G. G., Brambilla, R., Santos, J. H. Z., Fisch, A. G. J., Bioapplications for molecularly imprinted polymers. *Journal of Separation Science*, 36, p. 636-643 (2013).
- Mukherjee, I., Mylonakis, A., Guo, Y., Samuel, S. P., Li, S., Wei, R. Y., Effect of nonsurfactant template content on the particle size and surface area of monodisperse mesoporous silica nanospheres. *Microporous and Mesoporous Materials*, 122, 168-74 (2009).
- Nikolić, M., Giannakopoulos, K. P., Srdić, V. V., Synthesis and characterization of mesoporous silica core-shell particles. *Processing and Application of Ceramics*, 4, p. 81-85 (2010).
- Oliveira, D. M. F., Synthesis and characterization of nanostructured metal oxides and their use in nanocomposites with poly (vinyl alcohol). Thesis (State University of Maringá), Maringá (2009).
- Oliveira, D. L., Wilbey, R. A., Grandison, A. S., Roseiro, L. B., Natural caprine whey oligosaccharides separated by membrane technology and profile evaluation by capillary electrophoresis. *Food and Bioprocess Technology*, 7, p. 915-920 (2014).
- Ostroski, I. C., Dantas, J. H., Sehn Canavesi, R. L., Silva, E. A., Arroyo, P. A., Barros, M. A. S. D., Estudo da remoção do íon Fe (II) em colunas de leite fixo, utilizando-se a Zeólita NaY. *Acta Scientiarum Technology*, Maringá, 33, p. 305-312 (2011). (In Portuguese).
- Pradhan, S., Boopathi, M., Kumar, O., Baghel, A., Pandey, P., Mahato, T. H., Singh, B., Vijayaraghavan, R., Molecularly imprinted nanopatterns for the recognition of biological warfare agent ricin. *Biosensors and Bioelectronics*, 25, p. 592-598 (2009).
- Qu, F., Zhu, G., Huang, S., Li, S., Sun, J., Zhang, D., Qiu, S., Controlled release of Captopril by regulating the pore size and morphology of ordered mesoporous silica. *Microporous and Mesoporous Materials*, 92, p. 1-9 (2006).
- Relpius, C., Lactase, an optimum enzyme for low lactose dairy products. *Asia Pacific Dairy Industry*, p. 24-27 (2008).
- Seolatto, A. A., Câmara, M. M., Tavares, C. R., Cossich, E. S., Silva, E. A., Remoção de níquel(II) de soluções aquosas pela biomassa *Sargassum filipendula* em múltiplos ciclos de sorção-dessorção. *Acta Scientiarum Technology*, 31, p. 57-64 (2009). (In Portuguese).
- Silva, E. A., Cossich, E. S., Tavares, C. R. G., Filho, L. C., Guirardello, R., Modeling of copper(II) biosorption by marine alga *Sargassum* sp. in fixed bed. *Process Biochemistry*, 38, p. 791-799 (2002).
- Soares, C. M. F., Santos, O. A., Castro, H. F., Moraes, F. F., Zanin, G. M., Studies on immobilized lipase in hydrophobic sol-gel. *Applied Biochemistry and Biotechnology*, p. 113-116 (2004).
- Soares, C. M. F., Zanin, G. M., Moraes, F. F., Santos, O. A. A., Castro, H. F., Molecular imprinting of β -cyclodextrin/cholesterol template into a silica polymer for cholesterol separation. *Journal of Inclusion Phenomena and Macrocyclic Chemistry*, 57, p. 79-82 (2007).
- Suteewong, T., Sai, H., Bradbury, M., Estroff, L. A., Gruner, S. M., Wiesner, U., Synthesis and formation mechanism of aminated mesoporous silica nanoparticles. *Chemistry of Materials*, 24, p. 3895-3905 (2012).
- Tominaga, Y., Igawa, S., Asai, S., Sumita, M., Ion-conductive properties of mesoporous silica-filled composite polymer electrolytes. *Electrochimica Acta*, 50, p. 3949-3954 (2005).
- Turner, N. W., Jeans, C. W., Brain, K. R., Allender, C. J., Hlady, V., Britt, D. W., From 3D to 2D: A review of the molecular imprinting of proteins. *Biotechnology Progress*, 22, p. 1474-1489 (2006).
- Wanyika, H., Gatebe, E., Kioni, P., Tang, Z., Gao, Y., Synthesis and characterization of ordered mesoporous silica nanoparticles with tunable physical properties by varying molar composition of reagents. *African Journal of Pharmacy and Pharmacology*, 5, p. 2402-2410 (2011).
- Wei, Y., Xu, J., Dong, H., Dong, J. H., Qiu, K., Preparation and physisorption characterization of d-glucose-templated mesoporous silica materials via base-catalyzed sol-gel process. *Chemistry of Materials*, 11, p. 2023-2029 (1999).
- Whitcombe, M. J., Chianella, I., Larcombe, L., Piletsky, S. A., Noble, J., Porter, R., Horgan, A., The rational development of molecularly imprinted polymer-based sensors for protein detection. *Chemical Society Reviews*, 40, p. 1547-1571 (2011).